Journal of Organic Farming of Medicinal Plants: June 2025; 4 (1): 1-16
Available online at http://www.jofmp.areeo.ac.ir

Original Article

Green Synthesis of *Kelussia odoratissima* Silver Nanoparticles: A Comprehensive Assessment of Potent Antibacterial and Antioxidant Activities

Fahimeh Najafi[a], Samira Khadivi[b], Ehsan Rostami[b]

[a]*Department of Chemistry, Ro.C. Islamic Azad University, Roudehen, Iran.*
[b]*Department of Environment, Ro.C. Islamic Azad University, Roudehen, Iran.*

ARTICLE INFO

Corressponding Author:
Fahimeh Najafi
fahimeh@iau.ac.ir ,
fahimnajafi@gmail.com

Received: 4 September 2025
Accepted: 18 June 2026

Keywords:
Bioreduction
Phytochemical-mediated synthesis
Radical scavenging capacity
Minimum Inhibitory Concentration

ABSTRACT

This study reports the green synthesis of silver nanoparticles using an aqueous extract of Kelussia odoratissima as a reducing and stabilizing agent. The formation of spherical, crystalline nanoparticles with an average size of 178±12 nm was confirmed by spectroscopic, electron microscopy, and X-ray diffraction analyses. A positive zeta potential (+22.4 mV) indicated high colloidal stability, while FTIR spectra confirmed the role of plant phenolic compounds in the reduction and capping process. Biological activity assessment demonstrated that the synthesized nanoparticles possess significant and concentration-dependent antibacterial effects against Gram-negative (e.g., *Escherichia coli* and *Klebsiella pneumoniae*) and Gram-positive (e.g., *Staphylococcus aureus* and *Salmonella typhimurium*) pathogens. The Minimum Inhibitory Concentration (MIC) was lowest for *E. coli* (19.8 ± 0.1 µg/mL) and highest for *S. aureus* (174 ± 1.2 µg/mL). The MBC/MIC ratio primarily indicated a bactericidal effect against the Gram-negative bacteria. They also showed significant antioxidant capacity in DPPH and ABTS assays. Overall, this work demonstrates the efficacy of *K. odoratissima* extract in producing biogenic silver nanoparticles with favorable biological properties.

1. Introduction

Nanotechnology constitutes a transformative scientific frontier, fundamentally predicated on the manipulation of matter at the atomic and molecular scale. This domain is characterized by the emergence of size-dependent phenomena - including quantum confinement, surface Plasmon resonance, and markedly elevated surface-area-to-volume ratios - which confer materials with distinct optical, electronic, and catalytic properties not observable in their bulk counterparts. The discipline is inherently interdisciplinary, integrating principles from solid-state physics, colloidal chemistry, and materials science to enable the rational design of nanostructures with tailored functionalities. Advances in characterization methodologies, such as high-resolution transmission electron microscopy and X-ray photoelectron spectroscopy, have been instrumental in elucidating the structure-property relationships that underpin Nano scale behavior. The convergence of nanotechnology with biotechnology and biomedicine has catalyzed a paradigm shift in therapeutic and diagnostic strategies. This synergy has facilitated the development of sophisticated platforms, including targeted drug delivery systems, contrast agents for advanced imaging, and nanozymes with tailored catalytic activity. In antimicrobial applications, engineered nanomaterials leverage enhanced surface reactivity and functionalization capacity to disrupt microbial membranes and potentiate reactive oxygen species generation. Similarly, their antioxidant efficacy is often derived from surface-bound phytochemicals capable of efficient electron donation.(Bunggulawa et al.2018, Siddiqi et al.2018, Taghavizadeh yazdi et al.2020, Shamasi et al.2021, Aseyd Nezhad et al.2020, Taghavizadeh yazdi et al.2018, Zare zade et al.2018, Ashna et al.2020, Taghavizadeh yazdi et al.2019, Peña-Bahamonde et al.2018)

Silver nanoparticles (AgNPs) represent a quintessential model system in nanotechnology, demonstrating how the reduction of metallic silver to the Nanoscale confers emergent optical, catalytic, and biological properties not observed in its bulk form. Nanoparticle synthesis technology, especially silver nanoparticles, has catalyzed a paradigm shift in the development of advanced antibacterial and antioxidant materials.Thus, unlike traditional chemicals, engineered nanoparticles provide targeted delivery, sustained release kinetics, reduced propensity for microbial resistance and increased antioxidant properties. (Elemike et al.2018, Phull et al.2016)

Silver nanoparticle synthesis encompasses physical, chemical, and biological methodologies. Among these, green synthesis - utilizing plant extracts, microorganisms, or biological macromolecules - has garnered significant attention for its eco-friendly profile, cost-effectiveness, and inherent ability to produce nanoparticles with enhanced colloidal stability and bioactivity. This green synthesis approach not only eliminates the need for harsh reducing agents but also often results in nanoparticles capped with bioactive molecules, synergistically enhancing their functionality for biomedical and environmental applications. (Yasir et al.2018, Asif et al.2022)

Green synthesis of nanoparticles utilizing plant extracts capitalizes on the rich repertoire of phytochemicals-such as polyphenols, flavonoids, and terpenoids -which act as both reducing and stabilizing agents, and even increase antibacterial properties. Enabling efficient nanoparticle formation under ambient conditions without requiring high energy inputs or toxic chemicals. The elimination of extreme temperatures, pressures, and hazardous reagents not only reduces environmental impact but also simplifies purification processes and enhances biocompatibility. (Li et al.2011, Mirzaie et al.2017, Reidy et al.2013) The basic hypothesis of this study is that the use of mountain celery extract as a reducing/stabilizing agent in the synthesis of silver nanoparticles (AgNPs) will lead to the production of nanoparticles with a homogeneous size distribution (monodisperse) and a specific surface potential, whose bactericidal activity and free radical scavenging capacity are significantly better than those obtained by abiotic synthesis methods.

In recent years, extracts of various plants such as *ardaria draba (L.) Desv* or *Lepidium draba L* (Haji zadeh at al.2024), *Arthrospira subsalsa* (C. Agardh) Gomont (Babakhani et al.2024), *Rosa damascena Mill* flowers (Ercan et al.2024), and *Haplophyllum Obtusifolium* (Grachev) (Rezaei et al.2020) have been used to synthesize silver nanoparticles. In a seminal 2020 study, Rezaei et al. demonstrated the green synthesis of silver nanoparticles (AgNPs) using an X-ray-irradiated plant extract, systematically evaluating their antioxidant and antimicrobial properties. The biosynthesized AgNPs exhibited significant antibacterial efficacy against the Gram-negative pathogen *Klebsiella pneumoniae Mozaff*, likely attributable to the enhanced permeability of the outer membrane facilitating nanoparticle internalization and subsequent induction of oxidative stress. Conversely, no inhibitory effects were observed against the Gram-positive *Staphylococcus epidermidis* , suggesting structural resistance potentially mediated by the thicker peptidoglycan layer or altered surface charge interactions. Furthermore, antioxidant assessments via *DPPH* assay revealed a dose-dependent radical scavenging capacity, with efficacy correlating directly with nanoparticle concentration. (Rezaei et al.2020)

Iran’s unique biogeographical position and climatic heterogeneity have fostered exceptional diversity in its medicinal flora, including numerous endemic species. The genus *Kelussia* emerges as a taxon of special interest due to its distinctive phytochemical profile and ethnopharmacological relevance, warranting further investigation for potential pharmaceutical and nutraceutical applications. *Kelussia odoratissima*, a perennial aromatic species within the Apiaceae family and colloquially designated as “Kelussia” in Persian ethnobotanical nomenclature, thrives exclusively in high-altitude ecosystems of the central Zagros Mountains. Its distribution is constrained to elevations exceeding 2,500 meters above sea level, characterized by an annual precipitation regime of approximately 400 mm, predominantly in the form of seasonal snow cover. The species demonstrates narrow ecological amplitude, with primary endemic populations localized to the alpine regions of Kohrang, Bazaft, and Samsami Doab within the Chaharmahal and Bakhtiari provinces. Phytochemical profiling of Apium graveolens L. reveals two major classes of bioactive constituents: volatile essential oils and polyphenolic flavonoids. The essential oil fraction is characterized by a high abundance of phthalide derivatives, primarily butylidene dihydrophthalide and butylidene phthalide, which collectively account for approximately 70% of its total volatile composition. These phthalides exhibit significant pharmacological properties, functioning as dietary chemopreventive agents with demonstrated antitumor efficacy and protective effects against gastric ulcerogenesis. Concurrently, flavonoid compounds (localized predominantly in the seeds, stems, and inflorescences) display broad-spectrum therapeutic activities, including antiviral, antidiabetic, antihyperviscosity, hepatoprotective, and detoxification effects. (Rabbani et al.2011, Ghasemi et al.2011, Shahrani et al.2009, Kerry et al.1998)

Pharmacological evaluations have demonstrated that these phthalide derivatives exert significant antitumor effects against gastric malignancies, inhibiting tumor growth by approximately 67–83% in experimental models. The compounds also confer notable hepatoprotective properties, mitigating chemical-induced liver injury through modulation of detoxification enzymes and oxidative stress pathways. Ethnobotanical records indicate that traditional medicinal practices employ decoctions of the *Kelussia odoratissima* seeds and roots for the management of upper respiratory tract infections, severe cough, and inflammatory conditions such as rheumatism and gout. Additionally, aerial parts are utilized for gastrointestinal distress relief, further underscoring the plant's multifaceted therapeutic repertoire rooted in both empirical tradition and evidence-based bioactivity.(Ghasemi et al.2011, Shahrani et al.2009, Saeedi et al.2010) Furthermore, the phytochemical richness in volatile compounds and polyphenols, as exemplified by species like *Kelussia odoratissima*, renders such plants highly suitable for biogenic nanoparticle synthesis. Their bioactive constituents facilitate the fabrication of functionalized silver nanoparticles with enhanced antimicrobial, antioxidant, and therapeutic properties, highlighting their dual role as both phytotherapeutic agents and green mediators in nanotechnology. (Ghasemi et al.2011, Omidbaigi et al.2008)

This research systematically evaluated the synergistic antioxidant and antibacterial activities of aqueous extract of silver nanoparticles of *Kelussia odoratissima* against bacterial strains (designated as *Escherichia coli (ATCC 25922), Klebsiella pneumoniae (ATCC 13883), Staphylococcus aureus (ATCC 25923) and Salmonella typhimurium (ATCC 14028)*). The primary objective was to engineer a hybrid Nano bio-system by leveraging the unique physicochemical properties of silver nanoparticles and the inherent bioactivity of *Kelussia odoratissima* phytoconstituents. This approach aims to achieve maximal antioxidant and antimicrobial efficacy with minimal plant extract utilization, thereby optimizing resource efficiency while enhancing functional performance through Nano scale integration.

2. Materials and Methods

2.1 Plant collection and extraction

In this study, *Kelussia odoratissima* (*Kelussia odoratissima*) was collected in mid-spring (May) from the mountains of Kohrang County, Chaharmahal and Bakhtiari Province, and Taxonomic authentication was performed by systematic botanists at the Medicinal Plants Research Center, Shahrekord University of Medical Sciences (Herbarium Accession No: Skums.144)., and it was ultimately determined that this plant belongs to the *Apiaceae* family. After thorough cleaning and washing of *Kelussia odoratissima*, it was dried in the shade and then ground. For extraction of *Kelussia odoratissima*, the maceration was used; for this, 100 g of dried plant powder was added to 500 ml of deionized water and then this mixture was placed in a steam bath for 120 minutes to separate the primary extract to obtain the extract. Finally, the aqueous extract of *Kelussia odoratissima* was filtered using Whatman filter paper number 1 and a syringe filter and stored in Falcon tubes in dark glass jars at 4 °C (Prathap et al. 2014).

2.2 Synthesis and Characterization of Silver Nanoparticles

In this study, silver nanoparticles were synthesized through a biosynthesis method using water extract of *Kelussia odoratissima*. For this purpose, 15 ml of plant extract was added to 85 ml of silver nitrate solution with a concentration of 1 mM. In order to reduce silver ions, the prepared solution was kept for 24 hours at room temperature (25 °C) and in the dark. Due to the color change of the extract from pale yellow to dark brown to black, the production of silver nanoparticles was visible. After the regeneration process was completed, the extract containing nanoparticles was purified by centrifugation at 10,000 rpm for 30 min. The resulting precipitate was dried at 75°C for 6 h to obtain nanoparticle powder. The obtained silver nanoparticles were stored in microtubes at 4°C for further studies (Miri et al. 2019).

2.3 Investigation of Key Parameters Affecting Silver Nanoparticle Synthesis

2.3.1 Effect Effectiveness of pH

In order to optimize the pH value in the synthesis process of silver nanoparticles, five series of solutions containing 2.5 ml of mountain celery extract and 5 ml of silver nitrate solution with a concentration of 1 mM were prepared. Then, the pH of the solutions was adjusted to 4.8, 5.8, 6.8, 7.8, and 8.8, respectively, using 0.1M NaOH or 0.1M HCl solution. To evaluate the synthesized green nanoparticles, spectrophotometry was used to determine the optimal pH (Anuj et al. 2019, Shunki et al. 2004).

2.3.2 Effectiveness of Silver Nitrate Concentration

To investigate the effect of $AgNO_3$ concentration, 2 ml of different concentrations of silver nitrate solution (1 to 4 mM) were added to 2 ml of Kelussia odoratissima extract. Then, the pH of all these solutions was adjusted to the optimal pH to provide favorable biochemical conditions, and the ultraviolet (UV) spectrum of these produced solutions was measured and analyzed using a spectrophotometer to evaluate changes in the composition and biological activities of the extract. The results of these measurements were analyzed to determine the optimal concentration of silver nitrate (Shunki et al. 2004, Kumar et al. 2018).

2.4 Characterization of Synthesized Nanoparticles

In this research and investigation, after producing and optimizing two effective parameters, the properties of nanoparticles were investigated in detail using two analytical methods.

2.5 Electron Microscopy (SEM and TEM)

Scanning and transmission electron microscopes (Zeiss - EMIOC: SEM and TEM) were used to evaluate the size and shape of silver nanoparticles. In this regard, the precipitate obtained from the nanoparticles was centrifuged three times at 12,000 revolutions per minute (rpm). The precipitate obtained was then placed on a carbon-coated copper grid and, after drying with an infrared lamp, was photographed with an accuracy of 2.32 Ấ. Finally, the best nanoparticle in terms of size and shape was selected for the quality and efficiency of the produced nanoparticles.

2.6 Dynamic Light Scattering (DLS)

The hydrodynamic diameter and size distribution of the synthesized silver nanoparticles were rigorously characterized using dynamic light scattering (DLS) performed on a Zetasizer instrument. Measurements were conducted at a standard temperature of 25 °C, employing a coherent green laser source operating at a wavelength of 633 nm. DLS is a powerful, non-destructive physicochemical technique that quantifies the Brownian motion of particles suspended within a solution, whereby the velocity of this motion, expressed as the diffusion coefficient, is inversely proportional to the hydrodynamic particle size according to the Stokes-Einstein equation. This method is ideally suited for the rapid and precise determination of nanoparticle size distributions within a colloidal suspension, typically covering a broad size range from a few nanometers to several micrometers (Stetefeld et al. 2016).

2.7 Spectrophotometric Measurement

In order to qualitatively evaluate the s tabilizers around silver nanoparticles synthesized from *Kelussia odoratissima*, the absorption spectrum of the solutions was recorded using a Shimadzu UV-Visible spectrophotometer (UV- 1900) in the range of 200 to 900 nm. Based on the analysis of this spectrum, the most effective and best nanoparticle was selected.

2.8 Exploring Antioxidant

2.8.1 DPPH Free Radical Scavenging Ability Measurement

DPPH free radical undergoes a color change from purple to yellow by absorbing hydrogen from antioxidant compounds, which leads to a decrease in the absorption at a wavelength of 517 nm. (Swetha et al.2020) To perform this test, first 1 mg of DPPH powder was dissolved in 20 ml of ethanol and then 1 ml of it was added to 3 ml of a solution of silver nanoparticles of Kelussia odoratissima extract with concentrations of 50, 100, 200 and 400 μg/ml. Therefore, the final volume of the reaction mixture is 4 ml. The resulting solutions were incubated in the dark at room temperature for 30 minutes and finally their absorption was read at a wavelength of 517 nm by a spectrophotometer. Therefore, the absorbance measurements of the samples were performed against the control sample (negative control: ethanol) and the results were evaluated and compared with BHA as a positive control. The IC50 index, which indicates the concentration required to inhibit 50% of free radicals, is used as a criterion for measuring and evaluating the ability to inhibit free radicals (Vélez et al. 2018, Moshahary et al. 2020).

2.8.2 ABTS Radical Cation Decolorization Assay

The reactivity of ABTS ((2,2'-azino-bis(3-ethylbenzothiazoline-6-sulfonic acid) with antioxidant compounds is much higher than that of free radicals because the ABTS free radical is much more active and dynamic than DPPH, and for this reason this method is widely and extensive used. This method has unique features, including high reaction speed and greater sensitivity to other free radicals. In this method, ABTS radical is produced through the oxidation of potassium per sulfate and then the antioxidant activity of the samples is examined by measuring the changes in optical absorption at a wavelength of 734 nanometers (nm). At this wavelength, the maximum optical absorption of the produced radical is observed and the inhibition of the radical by antioxidant compounds will lead to a decrease in the optical absorption. To perform this experiment, first, stock solutions containing ABTS with a concentration of 7 mM and potassium per sulfate with a concentration of 2.45 mM were prepared. Then, by mixing the two stock solutions in equal proportions, the ABTS stock solution was prepared and to complete the reaction, this mixture was kept for 20 hours at room temperature (25 °C) and in the dark. After this period, the prepared solution was diluted with ethanol to obtain an optical absorption of 7.1 ± 0.01 at a wavelength of 734 nm. In the next step, 0.3 ml of different concentrations of extract nanoparticles and BHT (butylated hydroxytoluene) were added to 3 ml of the freshly prepared ABTS solution. After keeping the samples for 8 min in the dark, their optical absorption was measured at a wavelength of 734 nm. The percentage of radical inhibition was also calculated based on the changes in optical absorption (Ahmad et al. 2012, Kaur et al. 2019).

2.8.3 Antibacterial effectiveness of silver nanoparticles

To investigate the microbial properties of silver nanoparticles, a serial dilution method was used and replicated three times. Initially, standard bacteria including Escherichia coli (ATCC 25922), Klebsiella pneumoniae (ATCC 13883), Staphylococcus aureus (ATCC 25923), and Salmonella typhimurium (ATCC 14028) were prepared from a 24-hour pure culture in Luria-Bartoni agar liquid medium at 37°C. In order to standardize the concentration of bacteria and facilitate the evaluation of the effects of silver nanoparticles, in the first stage, bacterial colonies were harvested from the surface of the culture medium. And separately for each type of bacteria, a bacterial suspension equivalent to half McFarland was prepared using normal saline. To each well of a 96-well microplate, 5 µL of microbial suspension of different strains was added along with 95 µL of Mueller Hinton Broth liquid culture medium. Then, silver nanoparticles were added to all wells at various concentrations. The minimum inhibitory concentration (MIC) was defined as the lowest concentration capable of inhibiting bacterial growth (Salomoni et al. 2017, Zari et al. 2024).

2.9 Statistical analysis

All experiments were repeated in triplicate and the results were reported as mean ± standard deviation. Data analysis was performed using one-way analysis of variance (ANOVA).And comparison of means was performed using T-test, which was considered significant at the 0.05 level. In addition, SPSS and Excel software were used to draw graphs.

3. Results

3.1 Optimization of pH and Silver Nitrate Concentration for Nanoparticle

The aqueous extract of *Kelussia odoratissima* is known to be an effective reducing and stabilizing agent in the synthesis of silver nanoparticles. In Fig. 1, the first sign that is observed as confirmation of the synthesis of silver nanoparticles is the change in color of the solution from yellow to brown or tan. This color change indicates the formation of silver nanoparticles and the reducing activities of the *Kelussia odoratissima* extract.

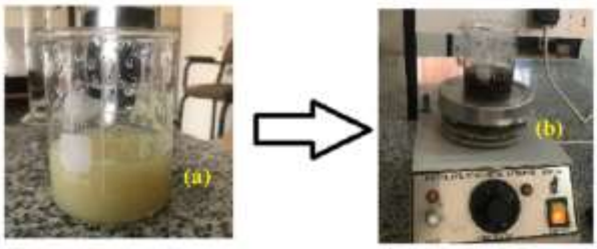

Fig.1. (a) Aqueous plant extract before reaction **(b)** Extract after addition of silver nitrate showing characteristic color change indicative of nanoparticle formation.

3.1.1 Optimizing the effectiveness of pH

After observing a color change to brown, indicating the success of nanoparticle synthesis, the pH of the final product was measured using a pH meter and recorded as 5.66. In order to more accurately analyze the effect of this key parameter on nanoparticle synthesis, pH values higher and lower than the initial value were also evaluated (Fig.2).

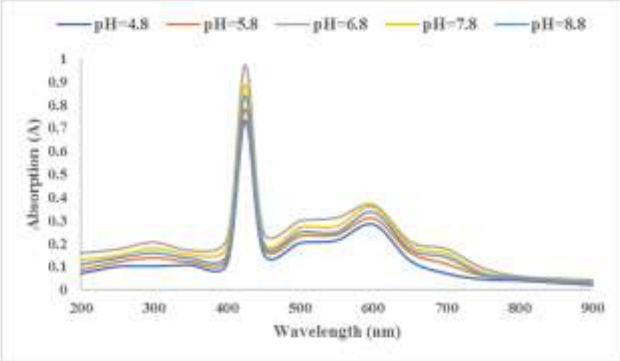

Fig.2. UV-Vis Absorption Spectra of Green-Synthesized AgNPs at Various pH Conditions.

3.1.2 Optimizing the effectiveness of silver nitrate concentration

The spectra recorded from the synthesized silver nanoparticles were studied using UV-Visible spectrophotometry at different concentrations of silver nitrate (1, 2, 3 and 4 mM). As can be seen in Fig. 3, with the gradual increase in the silver ion concentration, the absorption at 200 nm increased significantly and this trend continued up to a concentration of 4 mM. These results indicate that the optimal salt concentration for the synthesis of silver nanoparticles is 3 mM (Fig .3).

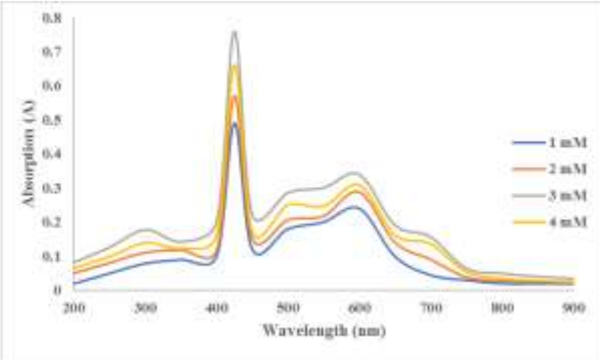

Fig.3. Silver Ion Concentration-Mediated Tuning of Plasmonic Properties in Green-Synthesized Silver Nanoparticles.

3.2 Morphological and Size Analysis by Electron Microscopy

To evaluate the size and morphology of the bio-synthesized silver nanoparticles, scanning electron microscopy (SEM) was used at a voltage below 30 kV and under vacuum pressure (10^{-5} Torr). Observations from SEM (Fig. 4) and TEM images clearly show that the synthesized silver nanoparticles mostly have spherical morphology. This feature indicates a controlled synthesis in which the biomolecular coating extracted from the *Kelussia odoratissima* extract uniformly inhibits crystal growth in all directions and prevents the formation of non-spherical nanostructures (such as nanoneedles or nanoplates). In addition to the spherical shape, it shows that the particle surface is smooth and free of structural irregularities.In quantitative analysis, the size distribution from the TEM images was performed on 100 individual particles (n=100). Based on these measurements, the average diameter of the biosynthesized silver nanoparticles is 178±12 nm. This value indicates that the average particle size is 178 nm and the standard deviation (SD) is 12 nm. This low standard deviation confirms the narrow size distribution in the sample, which indicates the high efficiency of the regenerating and stabilizing agents present in the *Kelussia odoratissima* extract.

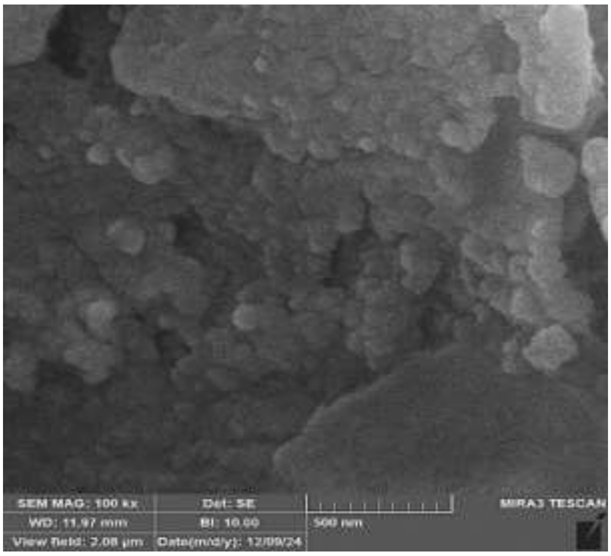

Fig. 4. SEM analysis of green-synthesized silver nanoparticles: Morphological characterization under optimized synthesis parameters.

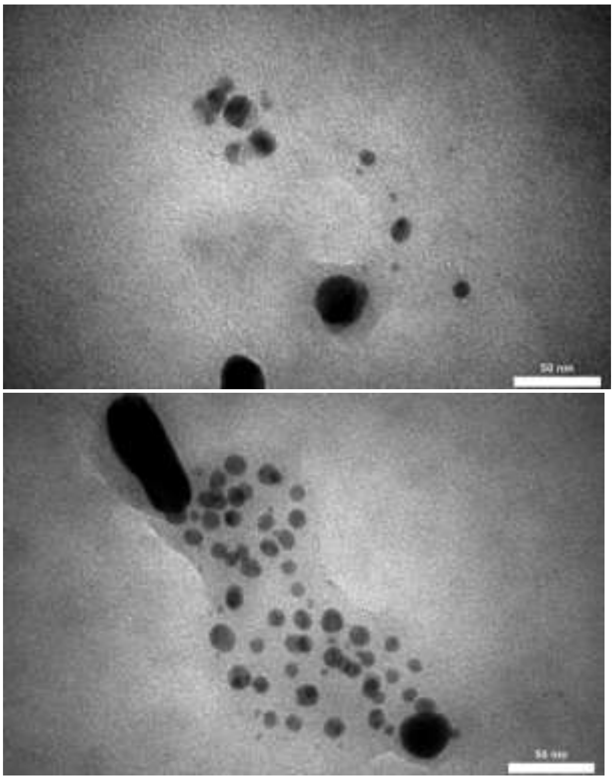

Fig. 5. Scanning transmission electron microscopy image of the synthetized nanoparticles by green-synthesized: Morphological characterization under optimized synthesis parameters.

3.3 Hydrodynamic Size and Surface Charge Analysis

The size, colloidal stability, and surface characteristics of the biogenic silver nanoparticles were assessed. Dynamic light scattering revealed a mean hydrodynamic diameter of 178 ± 12 nm, while zeta potential analysis indicated a value of +22.4 mV. This moderate positive charge denotes a colloidally stable suspension (Haghiralsadat et al. 2017, Jahanizadeh et al. 2017).

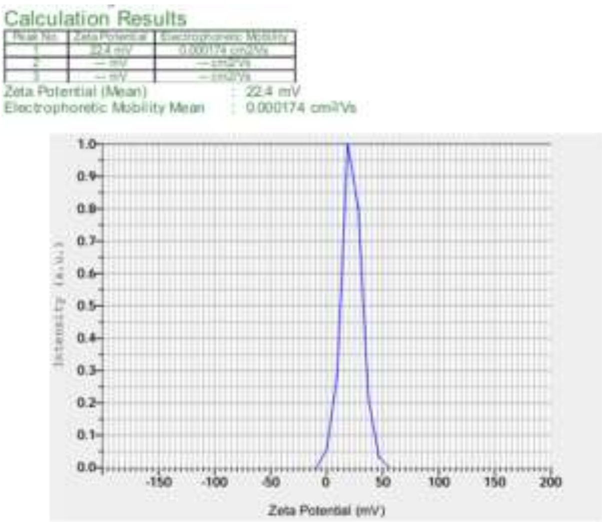

Fig. 6. Zeta potential distribution of biogenic silver nanoparticles: Colloidal stability analysis of *Kelussia odoratissima*-synthesized AgNPs in aqueous suspension.

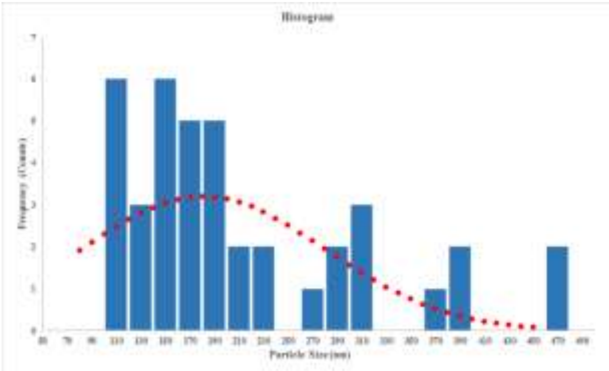

Fig. 7. Particle size distribution of silver nanoparticles synthesized with *Kelussia odoratissima* extract: Dynamic light scattering (DLS) analysis at 25°C.

3.4 Crystallographic Analysis (XRD)

The X-ray diffraction (XRD) pattern unequivocally confirms the successful synthesis of crystalline silver nanoparticles (AgNPs) with a face-centered cubic (fcc) structure. The diffraction peaks observed at 2θ values of 38.04°, 44.37°, 64.79°, and 77.78° are indexed to the (111), (200), (220), and (311) crystallographic planes of metallic silver (Ag^0), respectively. The intense and sharp nature of the predominant (111) peak, located at 38.04° with a full width at half maximum (FWHM) of 0.7872°.signifies a high degree of crystallinity and suggests a favorable crystal growth along this plane. The absence of any discernible peaks corresponding to silver oxide (e.g., Ag_2O or AgO) underscores the phase purity of the synthesized nanomaterial and the complete reduction of silver ions to their elemental state.

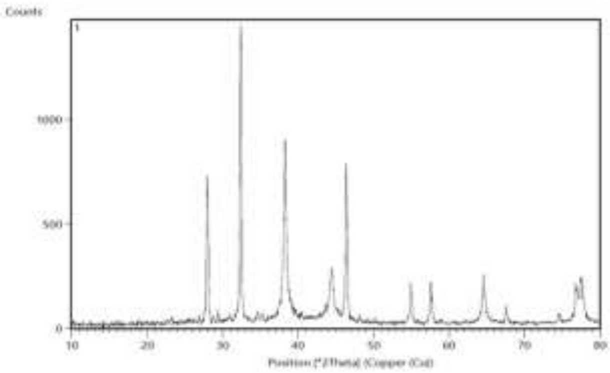

Fig. 8. Crystallographic characterization of biogenic silver nanoparticles: XRD analysis of *Kelussia odoratassima*-synthesized AgNPs revealing face-centered cubic structure.

Also, The remarkable agreement between the measured d-spacings (d_{111} = 2.36584 Å, d_{200} = 2.04162 Å, d_{220} = 1.43891 Å, d_{311} = 1.22689 Å) and the standard values for silver further corroborates the formation of the FCC phase. The calculated lattice parameter from these values is consistent with the known value for bulk silver ($a \approx$ 4.086 Å), indicating no significant lattice strain. The relative intensity ratio of the (111) to (200) peaks is considerably higher than that observed in the standard powder diffraction pattern, a phenomenon commonly observed in nanostructured silver due to the surface energy minimization that favors the exposure of the most stable (111) facets. This characteristic XRD profile, dominated by the (111) plane, is a sign of existence of phase-pure, crystalline silver nanoparticles.

3.5 Surface Functional Group Analysis (FTIR)

The Fourier-transform infrared (FTIR) spectroscopy analysis provided critical insights into the biomolecular capping and stabilization mechanisms of the synthesized silver nanoparticles (AgNPs) by *Kelussia odoratissima* extract. The spectrum exhibited characteristic vibrational modes of key functional groups from phytochemical constituents. A strong, broad absorption band at approximately 3435 cm^{-1} is attributed to O–H stretching vibrations of polyphenolic compounds and alcoholic groups, indicating the involvement of these hydrogen-bonding moieties in nanoparticle stabilization. Another prominent peak at 1554-1612 cm^{-1} corresponds to C=O stretching of carbonyl groups in quinones/flavonoids and C=C stretching in aromatic rings, confirming the role of tannins and polyphenolic antioxidants in reduction and surface functionalization. Additionally, the band at 1382.04 cm^{-1} is associated with O–H bending (phenolic) or C–H bending vibrations, further evidencing the organic coating derived from the plant extract. The identification of these functional groups on the nanoparticle surface conclusively demonstrates that phytoconstituents from *Kelussia odoratissima* extract (notably polyphenols and flavonoids) are integral to the reduction and stabilization processes.

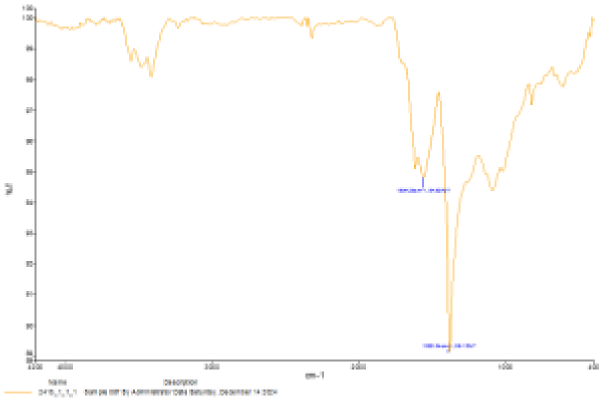

Fig. 9. Infrared (X) spectroscopy of *Kelussia odoratissima* aqueous extract.

3.6 Antibacterial Activity

The present study systematically evaluated the antibacterial efficacy of the synthesized nanoparticles against a panel of Gram-negative and Gram-positive pathogenic bacteria, including *Escherichia coli (ATCC 25922), Staphylococcus aureus (ATCC 25923), Salmonella typhimurium (ATCC 14028), and Klebsiella pneumoniae (ATCC 13883)*, utilizing the standardized disk diffusion assay. The results, as quantified in Table 2, unequivocally demonstrate a significant and broad-spectrum antibacterial activity associated with the tested nanoparticles. A clear, concentration-dependent response was observed, wherein the zones of inhibition exhibited a statistically significant expansion correlating with increasing nanoparticle concentration. This dose-dependent efficacy underscores the potent and predictable antimicrobial nature of the synthesized particles, suggesting their mechanism of action is scalable with dosage.

Notably, the antibacterial potency was found to be strain-specific. The most pronounced inhibitory effect was recorded against the Gram-negative bacterium *Escherichia coli*, which exhibited the largest zones of inhibition across the tested concentration range. Conversely, the Gram-positive bacterium *Streptococcus pneumoniae* displayed the highest degree of resistance, as evidenced by the smallest inhibition zones. This differential activity likely reflects variations in the complex architectural and compositional differences of the bacterial cell envelopes. The thick, multi-layered peptidoglycan structure of Gram-positive bacteria may present a more formidable barrier to nanoparticle penetration compared to the outer membrane of Gram-negative species, although the exceptional activity against *E. coli* suggests a potentially multifaceted mechanism beyond simple physical disruption.

Table 1. Crystallographic profile of biogenic silver nanoparticles: X-ray diffraction data indexing to face-centered cubic silver (JCPDS No. 01-076-1393) with corresponding interplanar spacings, and relative intensities.

Pos. [°2Th.]	Height [cts]	FWHM [°2Th.]	d-spacing [Å]	Rel. Int. [%]	Tip width [°2Th.]	Matched by
10.1496	18.33	0.3936	8.71548	3.97	0.4000	
27.5869	129.36	0.3936	3.23349	28.00	0.4000	
28.3551	103.91	0.4428	3.14761	22.49	0.4500	
31.9813	220.59	0.4920	2.79852	47.75	0.5000	01-076-1393
32.7717	226.44	0.3444	2.73280	49.02	0.3500	01-076-1393
33.1875	5.03	0.2460	2.69951	1.09	0.2500	01-076-1393
34.6957	15.59	0.7872	2.58554	3.37	0.8000	
38.0385	461.95	0.7872	2.36584	100.00	0.8000	01-076-1393
44.3714	183.97	0.7380	2.04162	39.82	0.7500	
46.7535	165.62	0.8364	1.94301	35.85	0.8500	01-076-1393
54.7315	79.36	0.7872	1.67716	17.18	0.8000	01-076-1393
57.8530	82.67	0.8364	1.59387	17.90	0.8500	01-076-1393
64.7936	126.29	0.8364	1.43891	27.34	0.8500	01-076-1393
67.8541	31.42	0.7380	1.38127	6.80	0.7500	01-076-1393
74.3422	16.67	0.6888	1.27597	3.61	0.7000	01-076-1393
77.7808	131.57	0.6000	1.22689	28.48	0.5000	

Table 2. Disk diffusion assay results demonstrating the antimicrobial efficacy of silver nanoparticles against a panel of bacterial strains.

Nanoparticle concentration ($\mu g/ml$)	Zone of Inhibition Diameter *(mm)*			
	Sal.typhimurium ATCC 14028	*E.Coli ATCC 25922*	*Pneumonia ATCC 13883*	*S.aureus ATCC 25923*
0	-	-	-	-
10	8.4 ± 0.85	8.9 ± 0.11	6.9 ± 0.85	7.9 ± 0.6
50	10.6 ± 0.14	11.9 ± 0.25	9.4 ± 0.27	9.9 ± 1.1
250	14.2 ± 0.47	16.7 ± 0.50	12.2 ± 0.44	14 ± 1.3
1250	17.20 ± 0.77	21 ± 0.91	14.9 ± 0.66	16.6 ± 1.7

Table 3. *MIC* values of bio-fabricated AgNPs against prevalent bacterial strains

MIC of silver nanoparticle of extract ($\mu g/ml$)	Type of bacteria			
	Sal.typhimurium ATCC 14028	*E.Coli ATCC 25922*	*Klebsiella Pneumonia ATCC 13883*	*S.aureus ATCC 25923*
	144 ± 0.85	19.8 ± 0.16	54.4 ± 0.41	174 ± 0.27

Table 4. *MBC* values of bio-fabricated AgNPs against target pathogens.

MBC of silver nanoparticle of extract ($\mu g/ml$)	Type of bacteria			
	Sal.typhimurium ATCC 14028	*E.Coli ATCC 25922*	*Klebsiella Pneumonia ATCC 13883*	*S.aureus ATCC 25923*
	431.9 ± 0.50	59.5 ± 0.72	163.4 ± 0.30	695 ± 0.91

Table 5. Antioxidant efficacy of biogenic AgNPs: DPPH and ABTS radical scavenging percentages.

Concentration (μg/mL)	AgNPs DPPH Inhibition (%)	AgNPs ABTS Inhibition (%)	BHT Inhibition DPPH (%)	BHT Inhibition ABTS (%)
50	69.9±0.19	49.1±0.10	37.2±0.44	33.7±0.19
100	80.6±0.11	58.1±0.52	53.8±0.29	49.9±0.21
200	86.8±0.26	74.5±0.22	70.4±0.33	66.5±0.16
400	94±0.40	91.3±0.38	79.8±0.17	76.9±0.27

3.7 Analysis of Minimum Inhibitory Concentration (MIC)

The quantitative assessment of the bacteriostatic potency of the bio-synthesized silver nanoparticles (AgNPs) was determined through the standardized broth microdilution method, with the results meticulously detailed in *Table 3*. The most prominent activity was observed against the Gram-negative pathogen *Escherichia coli (ATCC 25922)* with a very low *MIC* of 19.8 ± 0.1 μg/mL. This indicates a high degree of sensitivity and emphasizes the effectiveness of the nanoparticles against bacteria. Another Gram-negative strain, *Klebsiella pneumoniae (ATCC 13883)*, also showed significant sensitivity with an *MIC* of 54.4 ± 1.1 μg/mL.In contrast, higher *MIC* values were observed for the Gram-positive *Salmonella typhimurium (ATCC 14028)* and *Staphylococcus aureus (ATCC 25923)*, with 144 ± 1.8 μg/mL and 174 ± 1.2 μg/mL, respectively. This differential susceptibility pattern is in line with the general trend observed in the literature, where Gram-negative bacteria often show greater susceptibility to silver nanoparticles due to their thinner peptidoglycan layer, which may facilitate the penetration of nanoparticles and interaction with the cytoplasmic membrane.

The very low standard deviation associated with each *MIC* value (ranging from ±0.1 to ±1.8 µg/mL) confirms the excellent reproducibility and precision of the broth microdilution assay and confirms the robustness of the results obtained. The spectrum of activity, in particular the potent inhibition of *E. coli*, highlights the potential of these plant-synthesized AgNPs as promising antimicrobial agents against critical pathogenic strains.

As quantified in Table 4, the *MBC* analysis revealed a stark, strain-dependent bactericidal activity. For the Gram-negative strains, the *MBC* was determined to be 59.5 ± 0.72 µg/ml for *Escherichia coli (ATCC 25922)* and 163.4 ± 1.3 µg/ml for *Klebsiella pneumoniae (ATCC 13883)*. Notably, the exceptionally low MBC value against *E. coli* reinforces its high susceptibility observed in the *MIC* assays. For the Gram-positive *Staphylococcus aureus (ATCC 25923)*, the *MBC* was substantially higher at 695.0 ± 0.9 µg/ml. *Salmonella typhimurium (ATCC 14028)* exhibited an intermediate *MBC* value of 431.9 ± 1.5 µg/ml.

The calculated *MBC*/*MIC* ratios provide crucial insight into the mechanism of action. For *E. coli* and *K. pneumoniae*, the ratios were 3.0 and 3.0, respectively (*MBC* = 59.5/19.8; 163.4/54.4), which falls within the established bactericidal threshold (*MBC*/*MIC* ≤ 4). This confirms a predominantly bactericidal effect against these Gram-negative pathogens. In contrast, the ratio for *S. aureus* was 4.0 (*MBC*/*MIC* = 695.0/174.0), indicating a primarily bacteriostatic mode of action at lower concentrations, with bactericidal effects achieved only at significantly higher concentrations.

3.8 Analysis of Antioxidant Activity

The synthesized silver nanoparticles (AgNPs) were subjected to a rigorous evaluation of their free radical scavenging potential using two established in vitro assays, ABTS and DPPH, with the results quantitatively detailed in Table 5. The experimental results demonstrate a significant concentration-dependent antioxidant activity for the biogenic silver nanoparticles. In the ABTS radical cation decolorization assay, the nanoparticles exhibited substantial scavenging capacity, with inhibition increasing from 49.1 ± 0.10% at 50 µg/ml to 91.3 ± 0.38% at 400 µg/ml. This performance notably surpassed the standard antioxidant BHT (Butylated Hydroxytoluene), which showed 37.2 ± 0.44% and 79.8 ± 0.17% inhibition at corresponding concentrations.

The DPPH assay further confirmed the potent free radical scavenging activity, where inhibition rates increased progressively from 69.9 ± 0.19% at 50 µg/ml to 94.0 ± 0.40% at 400 µg/ml. The nanoparticles consistently outperformed BHT across all tested concentrations, with the most pronounced difference observed at 400 µg/ml. The enhanced activity at higher concentrations suggests their potential application in antioxidant-based therapies and protective systems.

4. Discussion

The synthesis of biogenic nanoparticles has garnered increasing attention in biomedical and biological sciences due to their enhanced biocompatibility and functional efficacy. Concurrently, growing awareness of green chemistry principles and biological processes has necessitated the adoption of environmentally benign approaches for producing non-toxic bionanomaterials. This paradigm shift emphasizes the use of sustainable, eco-friendly protocols that minimize hazardous waste and energy consumption while maximizing safety and scalability for therapeutic and diagnostic applications. (Elia et al.2014)

In particular, the emergence of nanosilver technology has revolutionized the development of antioxidant and antibacterial materials, offering significant advantages over conventional chemical agents, including enhanced biocompatibility and multifunctional properties. While traditional chemical synthesis methods for nanoparticles often suffer from limitations such as low production yields and high energy requirements, green synthesis approaches using plant-derived compounds offer a sustainable alternative that operates without the need for surfactants, harsh conditions, or external stabilizing agents. (Kavoosi et al.2017, Mittal et al.2013) In this study, silver nanoparticles were synthesized using aqueous extracts of mountain celery through a green synthesis approach, and their antioxidant and antibacterial properties were systematically evaluated. The synthesis mechanism relies on the reduction of silver ions and subsequent charge neutralization, a process that is completed within 24 h at room temperature, demonstrating the efficiency of this method and its independence from high-temperature reactions, which is in line with previously reported findings. (Sathyavathi et al.2010) Synthesis mechanism the high reduction potential of *Kelussia odoratissima* water extracts is attributed to their rich phytochemical composition, such as phthalides such as anthocyanidins and proanthocyanidins. Oxidation of functional groups such as hydroxyl, carbonyl, and aldehydes facilitates the reduction of silver ions, leading to the formation of stable silver nanoparticles. (Nikbakht et al.2016) A visible indicator of successful synthesis was the transition to a dark brown color in the reaction mixture (Fig.1), confirming the formation of predominantly spherical and crystalline silver nanoparticles - a result that is in line with previous studies. (Khane et al.2022) Further validation was provided by UV-Vis spectroscopy (Fig. 2) which revealed a distinct surface plasmon resonance peak at 400–430 nm, which is related to the collective oscillations of free electrons in silver nanoparticles. (Jegadeeswaran et al.2012).Thus, This study highlights the effectiveness of plant-mediated synthesis as a scalable, cost-effective, and environmentally sustainable route for the production of functional silver nanoparticles with promising antioxidant and antibacterial applications.

The pH of the reaction environment represents a critical parameter governing the nucleation, growth, and colloidal stability of biogenically synthesized nanoparticles. (Jegadeeswaran et al.2012) Previous studies have established that pH exerts limited influence on nanoparticle morphology but significantly modulates particle size and size distribution. In the present study, the pH of the reaction mixture following green synthesis was measured at 7.0 using a calibrated pH meter. Control experiments conducted at pH 4 demonstrated complete inhibition of nanoparticle formation, whereas increasing alkalinity progressively enhanced reduction efficiency. Maximum plasmonic absorption, indicating optimal nanoparticle yield and stability, was observed at pH 6.8, which was consequently established as the ideal pH for synthesis. Under alkaline conditions (pH > 7), extensive hydrolysis of silver ions (Ag^+) typically occurs, leading to the formation of stable silver hydroxide complexes (e.g., AgOH, $[Ag(OH)_2]^-$). These species exhibit reduced reactivity toward biological reducing agents, thereby inhibiting their participation in the nucleation and growth processes essential for nanoparticle formation. Consequently, the bioreduction efficiency is significantly diminished under highly basic conditions, highlighting the critical role of pH modulation in optimizing silver nanoparticle synthesis (Subhani at al. 2022).

Optimization of the volume parameter of the herbal extract is crucial for precise control over the morphology and efficiency of silver nanoparticles. It was observed that with increasing the volume of the extract, the intensity of surface plasmon absorption (SPR) increased directly and reached its maximum at a critical volume of 2 ml, which indicates the maximum efficiency of converting Ag+ ions into nanoparticles. This phenomenon is due to the simultaneous increase in the concentration of reducing agents (such as phenolic compounds) and stabilizing agents present in the aqueous phase; these agents promote burst nucleation kinetics. Deviation from this optimum point (concentration less than 2 ml) leads to incomplete reduction and at higher concentrations leads to insufficient stabilization of the surface of the nanoparticles. In both cases, the imbalance between reduction kinetics and stability will lead to an increase in particle size and a decrease in the overall quality of the final product. In this study, the size of the silver nanoparticles was obtained as 178±12 nm.

Similarly, variation in silver nitrate concentration revealed increased nanoparticle synthesis with higher Ag^+ ion availability, plateauing at 3 mM as the optimal concentration. Beyond this threshold, nanoparticle stability decreased precipitously, evidenced by a sharp decline in plasmon absorption due to colloidal aggregation. Temperature optimization studies indicated enhanced reaction kinetics up to 50°C, beyond which excessive molecular motion impeded nucleation and reduced nanoparticle concentration.

Reaction time emerged as another critical parameter, governing the completeness of the redox process between phytoconstituents and silver ions. Insufficient duration impaired full ion reduction, while prolonged intervals offered no further synthetic advantage. The optimal reaction time was determined to be 15 min, achieving near-complete reduction while maintaining operational efficiency. (Pryshchepa et al.2020)

The XRD pattern analysis exhibited distinct peaks at 2θ = 38.04°, 44.37°, 64.79°, and 77.78°, corresponding to the (111), (200), (220), and (311) lattice planes of face-centered cubic (FCC) silver . The observed peak broadening provides direct evidence of the nanoscale dimensions of the crystallites. This phenomenon arises from finite-size effects, wherein reduced crystal domain sizes result in constructive interference over narrower angular ranges. The preferential intensity enhancement of the (111) plane suggests anisotropic growth along this low-energy facet, a characteristic feature of biogenically synthesized silver nanoparticles. The absence of secondary phases (particularly silver oxide (Ag_2O)) validates the efficacy of the green synthesis route in producing phase-pure metallic silver nanostructures which aligns with established literature reports on biogenic silver nanostructures. (Salem et al.2020, Jebril at al.2020)

Morphological characterization through scanning and transmission electron microscopy (SEM/TEM) revealed well-dispersed, crystalline nanoparticles with predominantly spherical geometry. Quantitative image analysis established a narrow size distribution with a mean particle diameter of 178 ± 12 nm, demonstrating the efficacy of the synthesis protocol in controlling nucleation and growth processes. The observed crystallinity, evident from lattice fringes in high-resolution TEM, correlates directly with the distinct electron diffraction patterns and aligns with previous reports on biogenic silver nanostructures. This morphological homogeneity and crystallographic definition are critical for achieving reproducible surface plasmon resonance and enhanced bioactivity, as uniform particle geometry ensures consistent interaction with biological systems. The spherical morphology particularly facilitates optimal surface-to-volume ratios while minimizing anisotropic aggregation phenomena, thereby maximizing functional performance in biomedical applications. (Alahmad et al.2021)

In FTIR, the prominent broad absorption band at approximately 3435 cm^{-1} corresponds to O-H stretching vibrations, characteristic of polyphenolic compounds and alcoholic groups present in the plant extract. This intense absorption not only confirms the abundance of hydroxyl-rich compounds but also suggests their involvement in the stabilization process through hydrogen bonding interactions with nanoparticle surfaces. The significant shift in this band position compared to the pure plant extract indicates strong chemisorption of these polar functional groups onto the silver surface, effectively preventing aggregation through steric and electrostatic stabilization mechanisms. The critical spectral region between 1554-1612 cm^{-1} reveals two important vibrational modes: C=O stretching of carbonyl groups in quinones and flavonoids, and C=C stretching in aromatic rings. This dual functionality demonstrates the sophisticated chemical architecture of the reducing agents, where the carbonyl groups facilitate electron transfer for silver ion reduction while the aromatic systems provide structural stability through π-π interactions. The presence of these peaks strongly implicates tannins and polyphenolic antioxidants as primary actors in the bioreduction process, consistent with the known phytochemical profile of *K. odoratissima*. Furthermore, the distinct band at 1382 cm^{-1}, attributable to O-H bending vibrations in phenolic compounds or C-H bending modes, provides additional evidence of organic coating formation. This peak, often associated with the deformation vibrations of biomolecular capping agents, confirms the successful functionalization of nanoparticle surfaces with plant-derived phytochemicals .*Thus polyphenolic* compounds initiate silver ion reduction through electron donation from their hydroxyl and carbonyl groups, while subsequent stabilization is achieved through coordinated surface adsorption of multiple functional groups. The identified functional groups collectively contribute to enhanced nanoparticle stability and biological activity. The natural capping layer not only prevents aggregation but also potentially synergizes with the metallic core to enhance bioactivity, particularly in antioxidant applications where the combined effect of silver nanoparticles and phytochemical antioxidants could produce superior performance compared to either component alone. (Valsalam et al.2019, Göl et al.2020)

The most striking finding is the exceptional activity against Escherichia coli, evidenced by a remarkably low *MIC* of 19.8 ± 0.16 μg/ml and a corresponding *MBC* of 59.5 ± 0.72 μg/ml. The calculated MBC/*MIC* ratio of 3.0 definitively classifies the nanoparticles' action against this Gram-negative model as bactericidal. This potency is further corroborated by the disk diffusion assay, where *E. coli* exhibited the largest inhibition zones across all tested concentrations (e.g., 21.93 ± 0.50 mm at 1250 μg/ml). The exceptionally low *MIC*/*MBC* values, coupled with the substantial zone diameters, suggest a highly efficient mechanism of action against *E. coli*, likely involving rapid disruption of the outer membrane and subsequent interaction with intracellular components. A clear spectrum of susceptibility is evident from the data. Following *E. coli, Klebsiella pneumoniae* showed intermediate sensitivity (*MIC* = 54.4 ± 0.41 μg/ml; *MBC* = 163.4 ± 0.30 μg/ml), while the Gram-negative *Salmonella typhimurium* and the Gram-positive *Staphylococcus aureus* demonstrated the highest levels of resistance. This pattern (greater efficacy against Gram-negative bacteria) is a well-documented characteristic of silver nanoparticles. The observed differential susceptibility can be attributed to fundamental differences in cell envelope architecture. The thin peptidoglycan layer and presence of an outer membrane in Gram-negative bacteria may facilitate the adhesion and penetration of AgNPs, leading to membrane potential dissipation, protein denaturation, and eventual cell lysis. In contrast, the thick, multi-layered peptidoglycan sacculus of Gram-positive S. aureus likely acts as a more formidable physical and electrostatic barrier, necessitating higher concentrations for a bactericidal effect, as reflected in its *MBC*/*MIC* ratio of 4.0 and smaller inhibition zones.

A 2020 study examined the preparation of liposomes containing Hyssopus officinalis and Eryngium caeruleum M.Bieb and their antioxidant and antimicrobial properties. The study showed that the antioxidant activity of the extracts increased after encapsulation in nanoliposomes and among the bacteria studied, Streptococcus iniae and Staphylococcus aureus had larger growth inhibition zones, respectively.(Nouri.2020) In a 2024 study, Alyssum homolocarpum containing essential oils of Trachyspermum Copticum L and Teucrium polium L was used as a nanoemulsion. The antioxidant and antimicrobial activities of the nanoemulsion were obtained such that the size of the nanoparticles was 92.30 nm and the zeta potential was -12.19 mV. And a significant reduction in the total number of viable bacteria in the food was obtained. The nanoemulsions also had significant antioxidant properties. (Nouri.2024) In 2024, a study was conducted on the antimicrobial and antioxidant properties of silver nanoparticles in Datura extract. In this study, the optimal pH, optimal silver nanoparticle concentration, optimal extract volume, and optimal time were 6.5, 3 mM, 3 ml, and 10 min, respectively. The results showed that the highest antimicrobial effect was on E. coli bacteria and the lowest effect was on Streptococcus pneumoniae bacteria, and the antioxidant properties improved with increasing silver nanoparticle concentration. (Najafi et al.2024) In 2025, a study was conducted on the antimicrobial and antioxidant properties of silver nanoparticles from the aqueous extract of Hypericum perforatum. The antioxidant properties of the nanoparticles synthesized by ABTS and DPPH methods were concentration-dependent. The results showed that with increasing silver nanoparticle concentration, the antioxidant properties improved and the highest antibacterial activity was against standard strains of Listeria monocytogenes, Escherichia coli, Staphylococcus aureus and Salmonella enterica, respectively.(Najafi et al,2025) In 2022, a study was conducted to investigate the antioxidant, antimicrobial and anticancer potential of silver nanoparticles synthesized by tricolor violet extract, and the results showed that silver nanoparticles had strong antimicrobial effects. And MBC showed dose-dependent cytotoxicity of silver nanoparticles. Silver nanoparticles were able to inhibit the free radical scavenging effect of DDPH in a dose-dependent manner. (Hassanvand et al.2022)

The excellent concordance between the quantitative (*MIC*/*MBC*) and qualitative (disk diffusion) data significantly strengthens the validity of our findings. The perfect rank-order correlation in susceptibility (E. coli > K. pneumoniae > S. typhimurium ≈ S. aureus) across all three independent assays eliminates methodological artifacts and confirms the intrinsic antibacterial properties of the AgNPs. Furthermore, the low standard deviations associated with all reported values underscore the high reproducibility of both the synthesis protocol and the bioassays. The dose-dependent response observed in the disk diffusion assay, with inhibition zones expanding progressively from 10 to 1250 μg/ml, underscores the scalable nature of the antimicrobial effect. This predictable concentration-efficacy relationship is crucial for potential therapeutic applications, allowing for dosage calibration based on the target pathogen and infection severity. The bactericidal mechanism against key Gram-negative pathogens, confirmed by the low *MBC*/*MIC* ratios, positions these photosynthesized AgNPs as promising candidates for combating infections caused by multi-drug resistant Gram-negative bacteria, such as *E. coli* and *K. pneumoniae*, where conventional antibiotic options are increasingly limited. (Saka et al.2022, Kaur et al.2019, Joshi et al.2020)

Comparative analysis of biogenic silver nanoparticles (AgNPs) derived from diverse botanical sources (including *Rhododendron dauricum*, *Terminalia spp*., *Rosmarinus officinalis*, *Syzygium cumini*, *Canthium coromandelicum*, *Dalbergia rostrate*, *Fraxinus excelsior*, and *Cassia fistula*) has consistently demonstrated significant antioxidant activity. In alignment with these findings, the biosynthesized silver nanoparticles exhibited superior radical scavenging capacity in the *DPPH* assay compared to *ABTS* across all tested concentrations. Specifically, at 50 μg/mL, the AgNPs achieved 69.9% inhibition in *DPPH* compared to 49.1% in *ABTS*, with this performance advantage maintained throughout the concentration gradient, culminating in 94.0% (*DPPH*) versus 91.3% (*ABTS*) at 400 μg/ml. This enhanced performance in the *DPPH* assay, particularly evident at lower concentrations, suggests a more efficient hydrogen atom transfer (HAT) mechanism, which represents the primary reaction pathway for *DPPH* radical scavenging. The observed activity can be attributed to the distinct reaction mechanisms operative in each assay: while *DPPH* primarily involves HAT, the *ABTS* assay proceeds mainly through single electron transfer (SET). The molecular architecture of the phytoconstituent-capped AgNPs appears particularly optimized for hydrogen donation to the stable nitrogen-centered *DPPH* radical.

The antioxidant activity findings of silver nanoparticles (AgNPs) and the reference synthetic antioxidant BHT clearly show the superiority of AgNPs in DPPH and ABTS radical scavenging assays. As can be seen in Table 5, at the reference concentration of 400 μg/mL, silver nanoparticles have a 91±0.38% inhibition of ABTS radicals. This value is significantly higher than the inhibition performed by BHT at the same concentration, which is equal to 76.9±0.27%. Furthermore, it is observed that with increasing the concentration from 50 to 400 μg/mL, the ABTS inhibition efficiency for AgNPs increased from 49.1% to 91.3%. Also, in the DPPH method at a concentration of 400 μg/mL, nanoparticles show a 94.0±0.40% inhibition, while BHT at this concentration is 79.8±0.17%. This difference of 14.2% also confirms the superior performance of AgNPs in the DPPH assay. In this method, a dose-dependent response is also observed, similar to ABTS. This increased efficacy indicates synergistic interactions between the metallic silver core and the bioactive plant compounds of K. odoratissima, which may include flavonoids, phenolic acids, and other antioxidant compounds identified by FTIR analysis. The clear concentration-response relationship observed, coupled with the consistent outperformance of conventional antioxidants, positions these biogenic AgNPs as promising candidates for various biomedical applications requiring potent free radical scavenging activity, including oxidative stress mitigation and therapeutic interventions (Mohan et al. 2014, El –Rafie et al. 2014, Mittal et al. 2012, Bunghez et al. 2012, Oladipo et al. 2020).

5. Conclusion

Iran, endowed with diverse climatic zones and rich phytobiodiversity, possesses significant potential to emerge as a key contributor to the global medicinal plant trade. Among its unique endemic species, *Kelussia odoratissima* represents a rare and ecologically adapted pasture plant, thriving in semi-humid, high-altitude regions such as Isfahan, Chaharmahal-Bakhtiari, Kohgiluyeh-Boyerahmad, and Lorestan. The present study underscores the potential of *K. odoratissima* aqueous extract as a promising and sustainable source of natural antimicrobial and antioxidant agents for nutraceutical and pharmaceutical applications. However, the specific bioactive phytoconstituents responsible for its observed biological activities remain uncharacterized, highlighting a critical research gap. Further investigations should prioritize the bioactivity-guided isolation, purification, and structural elucidation of these compounds to delineate their mechanisms of action at the molecular level. Moreover, to the best of our knowledge, no prior study has explored the synthesis of silver nanoparticles using *Kelussia odoratissima* extract or comprehensively evaluated their synergistic antioxidant and antimicrobial efficacy. Thus, this work not only addresses an underexplored resource but also opens avenues for developing novel nanobiotechnological applications rooted in Iranian endemic botany. The integration of traditional knowledge with advanced nanotechnology may ultimately yield standardized, high-value herbal products capable of meeting international quality benchmarks and addressing growing global demand for natural therapeutics.

Acknowledgments
The authors would like to thank the Islamic Azad University, Roudehen Branch, for their moral support for this study.

References
Ahmad, N. & Sharma, S. (2012). Green synthesis of silver nanoparticles using extracts of Ananas comosus. GSC. 2(04), 141. https://doi.org/10.4236/gsc.2012.24020

Alahmad, A., Feldhoff, A., Bigall, N.C., Rusch, P., Scheper, T. & Walter, J.G. (2021). Hypericum perforatum L. -mediated green synthesis of silver nanoparticles exhibiting antioxidant and anticancer activities. Nanomaterials. 11(2), 487. https://doi.org/10.3390/nano11020487

Anuj, S.A., Gajera, H.P., Hirpara, D.G. & Golakiya, B.A. (2019). Bacterial membrane destabilization with cationic particles of nano-silver to combat efflux-mediated antibiotic resistance in gram-negative bacteria. Life Sciences. 230, 178-187. https://doi.org/10.1016/j.lfs.2019.05.072

Aseyd Nezhad, S., Es-Haghi, A. & Homayouni-Tabrizi, M. (2020). Green synthesis of cerium oxide nanoparticle using Origanum majorana L. leaf extract, its characterization and biological activities. Appl Organomet Chem. 34(2), e5314. https://doi.org/10.1002/aoc.5314

Ashna, M., Es-Haghi, A., Karimi Noghondar, M., Al Amara, D. & Taghavizadeh Yazdi, M.E. (2020). Greener synthesis of cerium oxide nanoemulsion using pollen grains of Brassica napus and evaluation of its antitumour and cytotoxicity properties. Mater Technol. 2020, 1-8. https://doi.org/10.1080/10667857.2020.1863558

Asif, M., Yasmin, R., Asif, R., Ambreen, A., Mustafa, M. & Umbreen, S. (2022). Green Synthesis of Silver Nanoparticles (AgNPs), Structural Characterization, and their Antibacterial Potential. Dose-response: a publication of International Hormesis Society. 20(1), 15593258221088709-15593258221088709. https://doi.org/10.1177/15593258221088709

Babakhani, M., Khaleghi, S. & Hajrasouliha, S. (2024). Investigating the Antioxidant and Antimicrobial Properties of Silver Nanoparticles Synthesized Using the Alcoholic Extract of Spirulina subsalsa Algae. Plant Biotechnology Persa. 6(1), 32-42. https://doi.org/10.61186/PBP.6.1.32

Bunggulawa, E.J., Wang, W., Yin, T., Wang, N., Durkan, C., Wang, Y. & et al. (2018). Recent advancements in the use of exosomes as drug delivery systems. J Nanobiotechnology. 16(1), 81. https://doi.org/10.1186/s12951-018-0403-9

Bunghez, I.R., Barbinta Patrascu, M.E., Badea, N.M., Doncea, S.M., Popescu, A. & Ion, R.M. (2012). Antioxidant silver nanoparticles green synthesized using ornamental plants. Journal of optoelectronics and advanced materials. 14(11), 1016.

Elemike, E., Onwudiwe, D.C., Ekennia, A. & Jordaan, A. (2018). Synthesis and characterisation of silver nanoparticles using leaf extract of Artemisi afra and them in vitro antimicrobial and antioxidant activities. IET Nanobiotechnol. 12(6), 722-726. https://doi.org/10.1049/iet-nbt.2017.0297

Elia, P., Zach, R., Hazan, S., Kolusheva, S., Porat, Z.E. & Zeiri, Y. (2014). Green synthesis of gold nanoparticles using plant extracts as reducing agents. International journal of nanomedicine. 20(9), 4007-4021. https://doi.org/10.2147/IJN.S57343

El-Rafie, H.M. & Hamed, M.A. (2014). Antioxidant and anti-inflammatory activities of silver nanoparticles biosynthesized from aqueous leaves extracts of four Terminalia species. Advances in Natural Sciences: Nanoscience and Nanotechnology. 5(3), 035008. DOI 10.1088/2043-6262/5/3/035008

Ercan, L. & Tükenmez, U. (2024). Antioxidant and Antimicrobial Properties of Different Silver Nanoparticles Produced by Green Synthesis. Current Perspectives on Medicinal and Aromatic Plants. 7(1), 12-23. https://doi.org/10.38093/cupmap.1434152

Ghasemi Pirbalouti, A., Shah Wali, A., Saghaee, S., Azizi, S., Hamedi, B. & Shahgholian, L. (2011). Effect of Chicory Extract (Cichorium intybus L.) and Cultivars of Bakhtiari Essences (Kelussia ordratassima Mizaff) on Removal of Organophosphoric Toxin Poisoning in Rat. Herbal Medicines. 2, 31-36.

Göl, F., Aygün, A., Seyrankaya, A., Gür, T., Yenikaya, C. & Şen, F. (2020). Green synthesis and characterization of Camellia sinensis mediated silver nanoparticles for antibacterial ceramic applications. Materials Chemistry and Physics. 250, 123037. https://doi.org/10.1016/j.matchemphys.2020.123037

Haghiralsadat, F., Amouabedini, G., Naderinezhad, S., Sheikhha, M.H., Malaei-balasi, Z., Akbarzadeh, A. & et al. (2017). An Evaluation of the Trans membrane Ammonium Sulfate Gradients Method In Lipid System to Improve Trapping Capacity of Amphipathic Weak. NCMBJ. 7(28), 49-60.

Hajizadeh, M., Sadeghian Sarayan, M. & et al. (2024). Evaluation of antimicrobial and antioxidant effects of silver nanoparticles synthesized with leaves of Lepidium draba L. Journal of Radiation Research and Applied Sciences. 17(3), 101004. https://doi.org/10.1016/j.jrras.2024.101004

Hassanvand, A., Saadatmand, S., Lari Yazdi, H. & Iranbakhsh, A.R. (2022). Investigation of Antioxidant, Antimicrobial and Anticancer Potential of Silver Nanoparticles synthesized by Viola tricolor L. Extract. Journal of Agricultural Science and Technology. 24(4), 885-900.

Jahanizadeh, S.H., Yazdian, F., Marjani, A., Omidi, M. & Rashedi, H. (2017). Curcumin- loaded Chitosan/ Carboxymethyl Starch/ Montmorillonite bio-Nano composite for reduction of dental bacterial biofilm formation. Int J Biolog Macromol. 105(Pt1), 757-763. https://doi.org/10.1016/j.ijbiomac.2017.07.101

Jebril, S., Jenana, R.K. & Dridi, C. (2020). Green synthesis of silver nanoparticles using Melia azedarach leaf extract and their antifungal activities: In vitro and in vivo. Materials Chemistry and Physics. 248, 122898. https://doi.org/10.1016/j.matchemphys.2020.122898

Jegadeeswaran, P., Shivaraj, R. & Venckatesh, R. (2012). Green synthesis of sil-ver nanoparticles from extract of Padina tetrastromatica leaf. Digest Journal of Nanomaterials and Biostructures. 7(3), 991-998.

Joshi, N.C., Joshi, E. & Singh, A. (2020). Biological Synthesis, Characterisations and Antimicrobial activities of manganese dioxide (MnO2) nanoparticles. Research Journal of Pharmacy and Technology. 13(1), 135-140. DOI: 10.5958/0974-360X.2020.00027.X

Kaur, A., Preet, S., Kumar, V., Kumar, R. & Kumar, R. (2019). Synergetic effect of vancomycin loaded silver nanoparticles for enhanced antibacterial activity. Colloids and Surfaces B:Biointerfaces. 176, 62-69. https://doi.org/10.1016/j.colsurfb.2018.12.043

Kaur, J., Gupta, N., Kaur, M. & Chatli, A.S. (2019). Antibacterial Effects of Green Synthesized AgNPs from Datura Metel Leaf Extracts. Int. J. Pure Appl. Biosci. 7, 247-252. http://dx.doi.org/10.18782/2320-7051.7327

Kavoosi, S. & Yaghoubi, H. (2017). [Synthesis of silver nanoparticles using green method of plant extract european marjoram (origanum majo-rana) and their antibacterial effects]. Journal of Cellular and Molecular Research. 30(2), 161-173.

Kerry, N. & Rice Evans, C. (1998). Peroxynitrite oxidices catechols to quinnones. Experimental & Molecular Biology Journal (FEBS Lett). 437(3), 167-171. https://doi.org/10.1016/S0014-5793(98)01223-X

Khane, Y., Benouis, K., Albukhaty, S., Sulaiman, G.M., Abomughaid, M.M., Al Ali, A. & et al. (2022). Green synthesis of silver nanoparticles using aqueous Citrus limon zest extract: Characterization and evaluation of their antioxidant and antimicrobial properties. Nanomaterials. 12(12), 2013. https://doi.org/10.3390/nano12122013

Kumar Sur, U., Ankamwar, B., Karmakar, S., Halder, A. & Das, P. (2018). Green synthesis of Silver nanoparticles using the plant extract of Shikakai and Reetha. Mater Today. 5(1), 2321-2329. https://doi.org/10.1016/j.matpr.2017.09.236

Li, X., Xu, H., Chen, Z.S. & Chen, G. (2011). Biosynthesis of nanoparticles by micro-organisms and their applications. Journal of Nanomaterials. 2011, 1-16. https://doi.org/10.1155/2011/270974

Miri, A., Mahdinejad, N., Ebrahimy, O., Khatami, M. & Sarani, M. (2019). Zinc oxide nanoparticles: biosynthesis, characterization, antifungal and cytotoxic activity. Materials Science and Engineering: C. 104, 109981. https://doi.org/10.1016/j.msec.2019.109981

Mirzaie, A., Bagheri, A.A., Noorbazargan, H. & Sadat Shandiz, S.A. (2017). The inhibitory effect of Artemisa quttensis extract on norA efflux pump in ciprofloxacin resistant Staphylococcus aureus strains using ethidium bromide and Real-Time PCR methods. Majallahi. Dānishgāhi. ʽUlūmi. Pizishkī. Qum. 11(10), 51-63.

Mittal, A.K., Chisti, Y. & Banerjee, U.C. (2013). Synthesis of metallic nanoparticles using plant extracts. Biotechnology Advances. 31(2), 346-356. https://doi.org/10.1016/j.biotechadv.2013.01.003

Mittal, A.K., Kaler, A. & Banerjee, U.C. (2012). Free Radical Scavenging and Antioxidant Activity of Silver Nanoparticles Synthesized from Flower Extract of Rhododendron dauricum. Nano Biomedicine & Engineering. 4(3), 118-124. DOI: 10.5101/nbe.v4i3.p118-124

Mohan, S.C., Sasikala, K., Anand, T., Vengaiah, P.C. & Krishnaraj, S. (2014). Green synthesis, antimicrobial and antioxidant effects of silver nanoparticles using Canthium coromandelicum leaves extract. Research Journal of Microbiology. 9(3), 142. DOI:10.3923/jm.2014.142.150

Moshahary, S. & Mishra, P. (2020). Synthesis of silver nanoparticles (AgNPs) using culinary banana peel extract for the detection of melamine in milk. Journal of Food Science and Technology. 58, 797-804. https://doi.org/10.1007/s13197-020-04791-x

Najafi, F. & Shafiei, Z. (2025). Investigating the antioxidant properties and antimicrobial activity of green synthesis of silver nanoparticle by using the aqueous extract of Hypericum perforatum. MEDICAL SCIENCES. 35(1), 24-34. DOI 10.61186/iau.35.1.24

Najafi, F., Shafiei, Z. & Mohammadzadeh, M. (2024). Evaluation of the antibacterial and antioxidant properties of green nanoparticles synthesized from the extract of Datura plant. Iran J Cult Health Promot. 7(4), 641-650. DOI 10.22034/7.4.17

Nikbakht, M.R., Soleimani, Z., Moravveji, S.A. & Esalatmanesh, K. (2016). Evalu-ating the effectiveness of Pistacia atlantica in the improvement of diabetic foot. Feyz. 20(4), 347-351.

Nouri, N. (2020). preparation of nanoliposomes containing Hyssopus officinalis L. and Eryngium caeruleum M.bieb extracts and investigate their antimicrobial and antimicrobial effects. J,Med.plants. 19(75), 118-131. DOI: 10.29252/jmp.19.75.118

Nouri, N. (2024). Nanoemulsions of Trachyspermum copticum L. and Teucrium polium L. essential oils incorporated with coating to extend fillet chicken storage. Journal of Food Measurement and Characterization. 18, 4034-4046. https://doi.org/10.1007/s11694-024-02474-1

Oladipo, I.C., Lateef, A., Azeez, M.A., Asafa, T.B., Yekeen, T.A. & Ogunsona, S.B. (2020). Characterization and biomedical application of phytosynthesized gold nanoparticles from Datura stramonium seed extract. InIOP Conference Series: Materials Science and Engineering. 805(1), 012021. DOI 10.1088/1757-899X/805/1/012021

Omidbaigi, R., Sefidkon, F. & Saeedi, K. (2008). Essential Oil content and composition of Kelussia odoratissima Mozaff. As an Iranian endemic plant. J Essent Oil Bearing Plants. 11(6), 594-597.

Peña-Bahamonde, J., Nguyen, H.N., Fanourakis, S.K. & Rodrigues, D.F. (2018). Recent advances in graphene-based biosensor technology with applications in life sciences. J Nanobiotechnology. 16(1), 75. https://doi.org/10.1186/s12951-018-0400-z

Phull, A.R., Abbas, O., Ali, A., Raza, H., Jakim, S., Zia, M. & et al. (2016). Antioxidant, cytotoxic and antimicrobial activities of green synthesized silver nanoparticles from crude extract of Bergenia ciliate. Future J Pharm Sci. 3, 1-36. https://doi.org/10.1016/j.fjps.2016.03.001

Prathap, M., Alagesan, A. & Ranjitha Kumari, B.D. (2014). Anti - bacterial activities of silver nanoparticles synthesized from plant leaf extract of Abutilon indicum (L.) Sweet. J Nanostruct Chem. 4, 106. https://doi.org/10.1007/s40097-014-0106-1

Pryshchepa, O., Pomastowski, P. & Buszewski, B. (2020). Silver nanoparticles: Synthesis, investigation techniques, and properties. Advances in Colloid and Interface Science. 284, 102246. https://doi.org/10.1016/j.cis.2020.102246

Rabbani, M., Sajjadi, S.E. & Sadeghi, M. (2011). Chemical composition of the essential oil from Kelussia odoratissima Mozaff and the evaluation of its sedative and anxiolytic effects in mice. Clinics (Sao Paulo). 66(5), 843-848. https://doi.org/10.1590/S1807-59322011000500022

Reidy, B., Haase, A., Luch, A., Dawson, K.A. & Lynch, I. (2013). Mechanisms of silver nanoparticle release, transformation and toxicity: a critical review of current knowledge and recommendations for future studies and applications. Materials. 6(6), 2295-2350. https://doi.org/10.3390/ma6062295

Rezaei, M.R., Es-haghi, A., Yaghmaei, P. & Ghobeh, M. (2020). Assessment of Antioxidant and Antimicrobial Activities of Silver Nanoparticles Biosynthesized by Haplophyllum Obtusifolium. Avicenna Journal of Medical Biochemistry. 8(2), 94-98. https://doi.org/10.34172/ajmb.2020.14

Saeedi, K. & Omidbeigi, R. (2010). Chemical characteristics of the seed of Iranian endemic plant Kelussia odoratissima. Chemistry of Natural Compounds. 46(5), 813-815. https://doi.org/10.1007/s10600-010-9754-7

Saka, A., Jule, L.T., Gudata, L., Gindaba, A., Abdisa, S.S., Nagaprasad, N. & Ramaswamy, K. (2022). Green Synthesis of Datura stramonium (Asaangira) Leaves Infusion for Antibacterial Activity through Magnesium Oxide (MgO) Nanoparticles. Advances in Materials Science and Engineering. 1, 1-8. https://doi.org/10.1155/2022/7134991

Salem, S.S., El -Belely, E.F., Niedbała, G., Alnoman, M.M., Hassan, S.E., Eid, A.M. & et al. (2020).

Bactericidal and in -vitro cytotoxic efficacy of silver nanoparticles (Ag -NPs) fabricated by endophytic actinomycetes and their use as coating for the textile fabrics. Nanomaterials. 10(10), 2082. https://doi.org/10.3390/nano10102082

Salomoni, R., Léo, P., Montemor, A.F., Rinaldi, B.G. & Rodrigues, M. (2017). Antibacterial effect of silver nanoparticles in Pseudomonas aeruginosa. Nanotechnol Sci Appl. 10, 115-121. https://doi.org/10.2147/NSA.S133415

Sathyavathi, R., Krishna, M.B., Rao, S.V., Saritha, R. & Rao, D.N. (2010). Biosynthe-sis of silver nanoparticle susing Coriandrum sativum leaf extract and their application in nonlinear optic. Advanced science letters. 3(2), 138-143. https://doi.org/10.1166/asl.2010.1099

Shahrani, M., Pilehvarian, A., Kheyri, S., Asgari, A., Farokhi, E., Parvin, N. & et al. (2009). Effects of Kelussia odoratissima Mozaffarian (KOM) extract on blood lipid in Balb/c mice. Shahrekord University of Medical Sciences J. 10(4), 50-56.

Shamasi, Z., Es-Haghi, A., Taghavizadeh Yazdi, M.E., Amiri, M.S. & Homayouni-Tabrizi, M. (2021). Role of Rubia tinctorum in the synthesis of zinc oxide nanoparticles and apoptosis induction in breast cancer cell line. Nanomed J. 8(1), 65-72.

Shunki, S.S., Re, A., Ankamwar, R., Singh, A., Ahmad, A. & Sastry, M. (2004). Biological synthesis of trangular gold nanprisms. Nature Mat. 3(7), 482. https://doi.org/10.1038/nmat1152

Siddiqi, K.S., Husen, A. & Rao, R.A.K. (2018). A review on biosynthesis of silver nanoparticles and their biocidal properties. J Nanobiotechnology. 16(1), 14. https://doi.org/10.1186/s12951-018-0334-5

Stetefeld, J., McKenna, S.A. & Patel, T.R. (2016). Dynamic light scattering: A prac-tical guide and applications in biomedical sciences. Biophysical Re-views. 8(4), 409-427. https://doi.org/10.1007/s12551-016-0218-6

Subhani, M.A., Irshad, M., Nazir, A., Hafeez, M. & Ali, S. (2022). Synthesis and antibacterial potential of Loranthus pulverulentus conjugated silver nanoparticles. Microscopy Research and Technique. 85(11), 3530-3540. https://doi.org/10.1002/jemt.24204

Swetha, V., Lavanya, S., Sabeena, G., Pushpalaksmi, E., Jenson, S.J. & Annadurai, G. (2020). Synthesis and characterization of silver nanoparticles from Ashyranthus aspera extract for antimicrobial activity studies. Journal of Applied Sciences and Environmental Management. 24(7), 1161-1167. https://dx.doi.org/10.4314/jasem.v24i7.6

Taghavizadeh Yazdi, M.E., Amiri, M.S., Akbari, S., Sharifalhoseini, M., Nourbakhsh, F., Mashreghi, M. & et al. (2020). Green synthesis of silver nanoparticles using Helichrysum graveolens for biomedical applications and wastewater treatment. BioNanoScience. 10(4), 1121-1127. https://doi.org/10.1007/s12668-020-00794-2

Taghavizadeh Yazdi, M.E., Hamidi, A., Amiri, M.S., Kazemi Oskuee, R., Hosseini, H.A., Hashemzadeh, A. & et al. (2019). Eco-friendly and plant-based synthesis of silver nanoparticles using Allium giganteum and investigation of its bactericidal, cytotoxicity, and photocatalytic effects. Mater Technol. 34(8), 490-497. https://doi.org/10.1080/10667857.2019.1583408

Taghavizadeh Yazdi, M.E., Khara, J., Sadeghnia, H.R., Esmaeilzadeh Bahabadi, S. & Darroudi, M. (2018). Biosynthesis, characterization, and antibacterial activity of silver nanoparticles using Rheum turkestanicum shoots extract. Res Chem Intermed. 44(2), 1325-1334. https://doi.org/10.1007/s11164-017-3169-z

Valsalam, S., Agastian, P., Arasu, M.V., Al-Dhabi, N.A., Ghilan, A.K., Kaviyarasu, K., Ravindran, B., Chang, S.W. & Arokiyaraj, S. (2019). Rapid biosynthesis and characterization of silver nanoparticles from the leaf extract of Tropaeolum majus L. and its enhanced in -vitro antibacterial, antifungal, antioxidant and anticancer properties. Journal of Photochemistry and Photobiology B: Biology. 191, 65-74. https://doi.org/10.1016/j.jphotobiol.2018.12.010

Vélez, E., Campillo, G., Morales, G., Hincapié, C., Osorio, J. & Arnache, O. (2018). Silver Nanoparticles Obtained by Aqueous or Ethanolic Aloevera Extracts : An Assessment of the Antibacterial Activity and Mercury Removal Capability. J Nanomater. 2018, 1-7. https://doi.org/10.1155/2018/7215210

Yasir, M., Singh, J., Tripathi, M.K., Singh, P. & Shrivastava, R. (2018). Green Synthesis of Silver Nanoparticles Using Leaf Extract of Common Arrowhead Houseplant and Its Anticandidal Activity. Pharmacogn Mag. 13(Suppl 4), 840-844.

Zarezade, V., Moludi, J., Mostafazadeh, M., Mohammadi, M. & Veisi, A. (2018). Antioxidant and hepatoprotective effects of Artemisia dracunculus against CCl(4)-induced hepatotoxicity in rats. Avicenna J Phytomed. 8(1), 51-62.

Zari, N. & Nouri, M. (2024). Microbial, technological and probiotic traits of doogh enriched with natamycin and cinnamon essential oil loaded into nanoemulsion/lactobacillus strain. Iran.J.Chem.Eng. 43(8), 3113-3126.